

Electronic Supplementary Material

Alkylation of benzene with carbon dioxide to low-carbon aromatic hydrocarbons over bifunctional Zn-Ti/HZSM-5 catalyst

Xiangyu Liu¹, Yanling Pan², Peng Zhang¹, Yilin Wang¹, Guohao Xu¹, Zhaojie Su¹, Xuedong Zhu (✉)¹, Fan Yang (✉)¹

¹ Engineering Research Center of Large-Scale Reactor Engineering and Technology, Ministry of Education, East China University of Science and Technology, Shanghai 200237, China

² Department of Product Engineering, School of Chemical Engineering, East China University of Science and Technology, Shanghai 200237, China

E-mails: xdzhu@ecust.edu.cn (Zhu X); yfan0227@qq.com (Yang F)

Table S1. Catalysts Activities of carbon dioxide to aromatics

Catalyst	Temperature /K	Pressure /Mpa	H ₂ /CO ₂	GHSV /h ⁻¹	CO ₂ conversion /%	Aromatics selectivity /%	Ref.
ZnO/ZrO ₂ -ZSM-5	613	3	3	1800	9.0	70	4
ZnAlO _x -H-ZSM-5	593	3	3	6000	9.1	73.9	5
In ₂ O ₃ /HZSM-5	613	3	3	9000	13.1	78.6	6

Table S2. Distribution of products in liquid phase under different conditions

Temperature /K	Pressure /Mpa	H ₂ /CO ₂ /	GHSV /h ⁻¹	Benzene conversion /%	Selectivity/%				Phenyl ring yield ^a /%
					Toluene	Xylene	Ethylbenzene	C ₉ ⁺	
623	3	3:1	9000	6.9	89.1	8.5	1.0	1.4	98.6
673	3	3:1	9000	19.6	79.5	15.5	2.0	3.0	95.8
698	3	3:1	9000	22.4	76.0	18.2	2.1	3.7	95.1
748	3	3:1	9000	22.2	77.5	17.9	2.1	2.5	95.2
698	2	3:1	9000	18	81.1	14.4	1.8	2.7	96.2
698	4	3:1	9000	35.5	75.7	9.1	1.1	14.1	91.9
698	3	1:1	9000	10.6	84.9	8.5	3.5	3.1	97.8
698	3	2:1	9000	19.1	82.7	11.5	2.8	3.0	96.0
698	3	4:1	9000	26.3	73.4	20.3	2.2	4.1	94.2
698	3	3:1	6000	23.7	75.6	16.2	3.4	4.8	94.8
698	3	3:1	7500	21.9	79.2	14.7	2.2	3.9	95.3
698	3	3:1	12000	17.2	80.6	14.5	2.0	2.9	96.4
698	3	3:1	18000	15.3	76.4	17.5	2.1	4.1	96.6

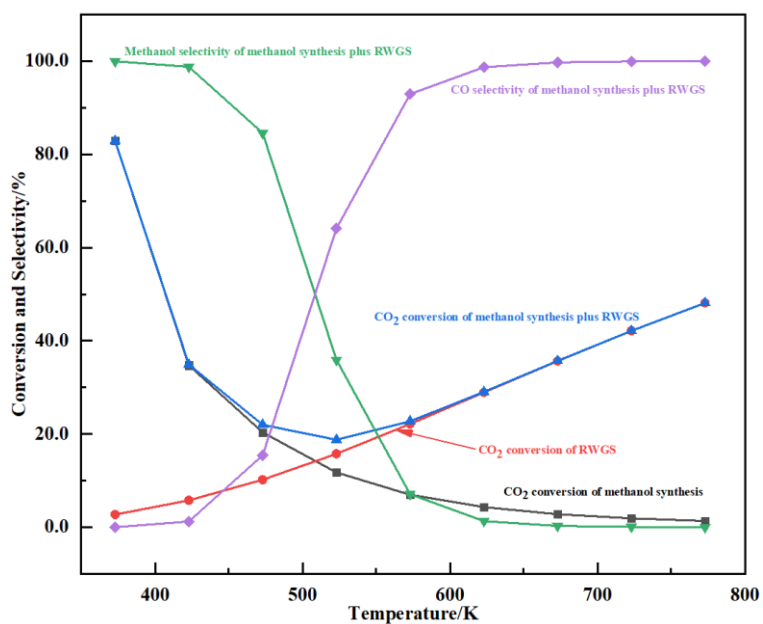


Fig. S1 Effects of temperature on the methanol synthesis by hydrogenation of Carbon dioxide and RWGS

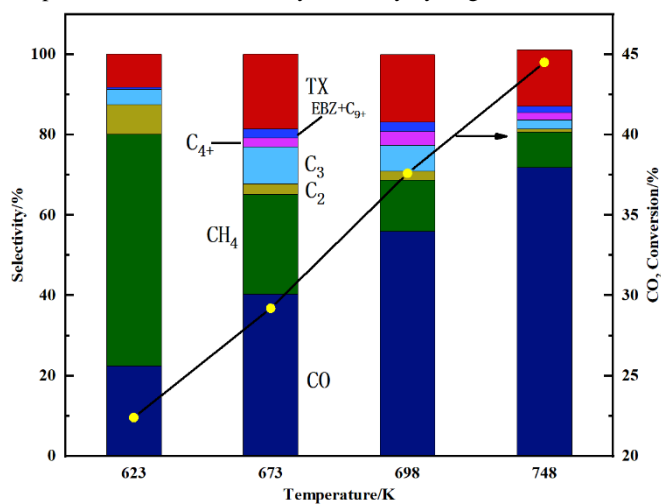


Fig. S2 Effects of temperature on CO₂ conversion and product selectivity based on CO₂

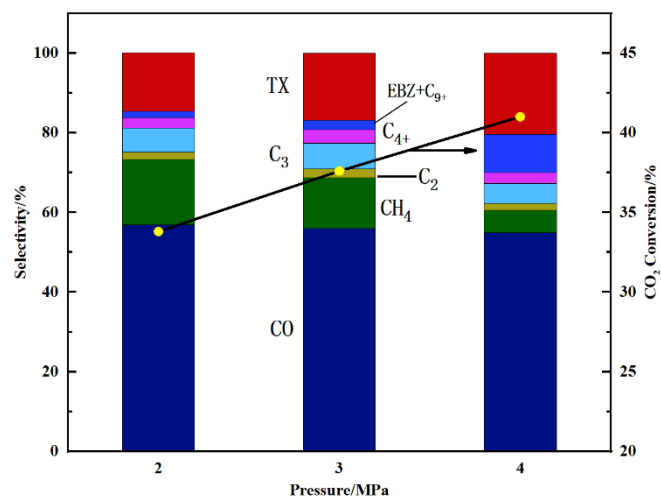


Fig. S3 Effects of pressure on CO₂ conversion and product selectivity based on CO₂

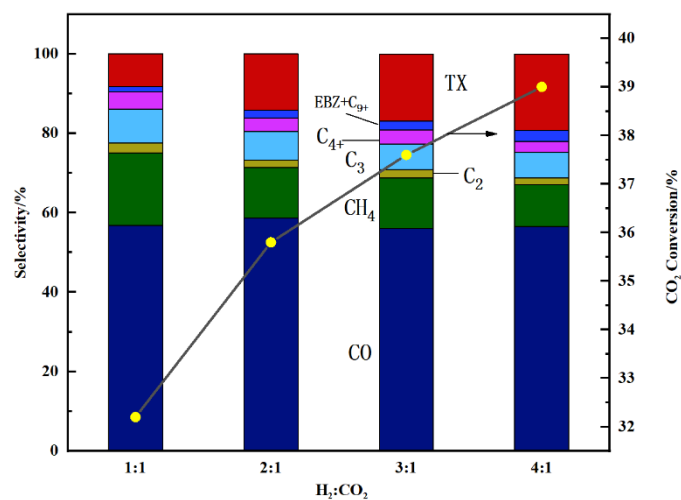


Fig. S4 Effects of feed ratios on CO₂ conversion and product selectivity based on CO₂

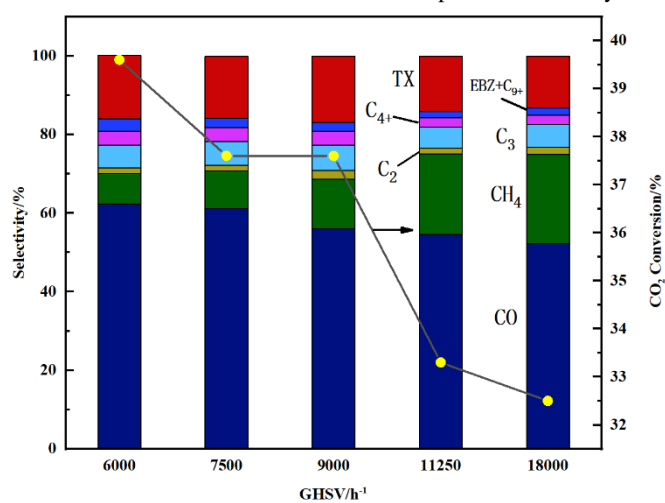


Fig. S5 Effects of GHSV on CO₂ conversion and product selectivity based on CO₂

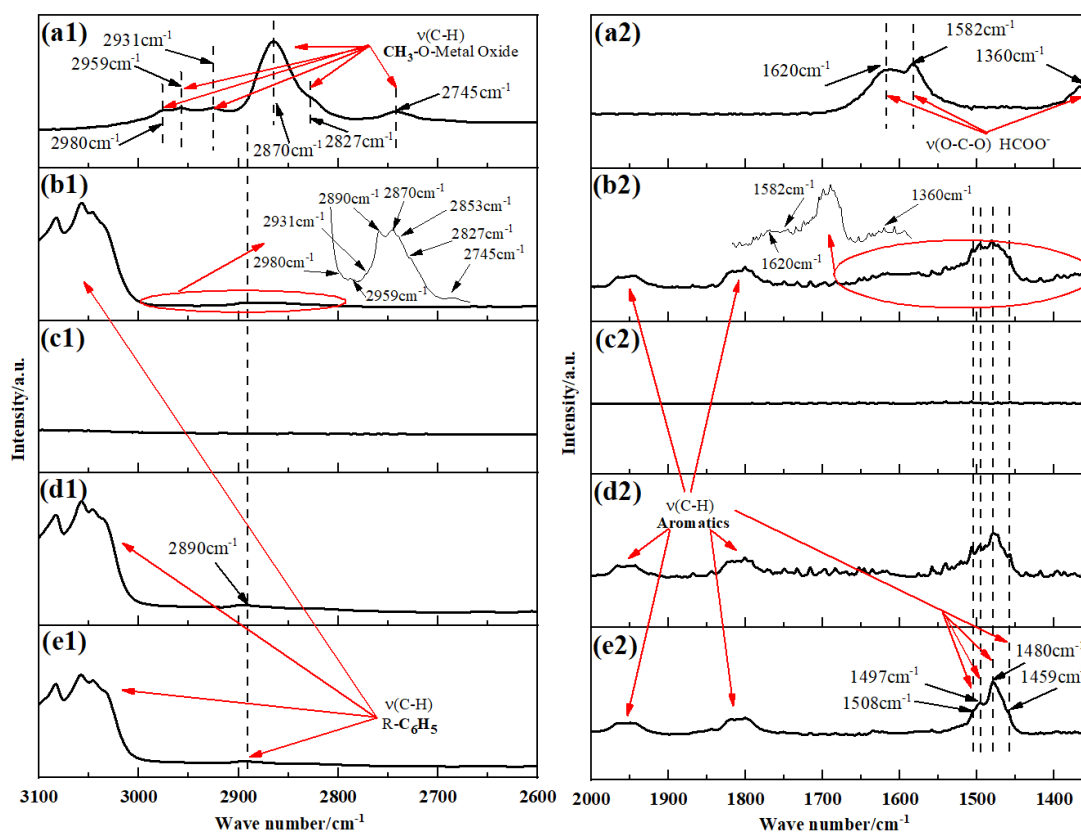


Fig. S6 In-situ IR spectra of $Zn_{0.1}Ti$, HZSM-5(13.5) recorded at 598 K under 6 atm. (a1,a2) Mixture of CO_2 and H_2 (10 ml/min, $H_2:CO_2=3:1$) is introduced into in-situ pool (325 °C and 6 atm) containing $Zn_{0.1}Ti$ oxide for 30 min. Then, the pool is swept by argon gas for 10 min; (b1,b2) After the last experiment step, benzene vapor is carried by argon(10 ml/min) into the in-situ pool; (c1,c2) Mixture of CO_2 and H_2 (10 ml/min, $H_2:CO_2=3:1$) is introduced into in-situ pool containing HZSM-5(13.5) under the condition which is same as step (a1,a2); (d1,d2) After the last experiment step, benzene vapor is introduced into the in-situ pool along with argon; (e1,e2) Benzene vapor is carried by argon(10 ml/min) into the in-situ pool including the $Zn_{0.1}Ti$ -HZ5(13.5) catalyst. The reaction conditions are the same as above

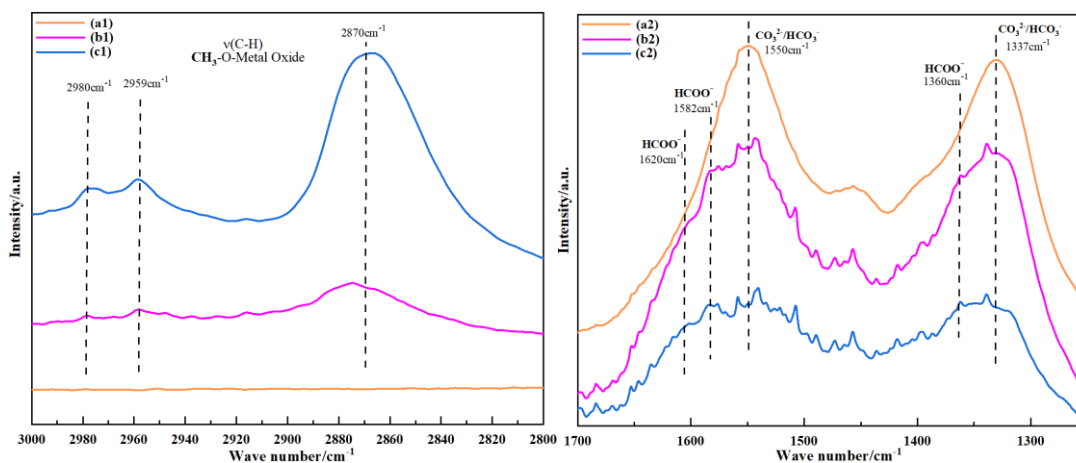


Fig. S7 In-situ IR spectra on the $Zn_{0.1}Ti$ oxide recorded at 598 K under 6 atm. (a1,a2) CO_2 (10ml/min) is pumped into the in-situ pool containing $Zn_{0.1}Ti$ oxide for 20 min; (b1,b2) Then, hydrogen (10ml/min) is introduced into the in-situ pool. The infrared spectrum is recorded at 10 min; (c1,c2) The infrared spectrum is recorded at 20 min after the introduction of hydrogen